Journal of Thermal Analysis and Calorimetry, Vol. 85 (2006) 1, 91–98

DEVELOPMENT AND USE OF A TG-DTA-MICROSCOPE FOR EVALUATION OF PHARMACEUTICAL MATERIALS

*Carol L. Grundner**, *Kate B. Poiesz and Nancy L. Redman-Furey*

Procter & Gamble Pharmaceuticals, Inc., P.O. Box 191, Norwich, New York 13815, USA

The successful combination of microscopy with thermogravimetry-differential thermal analysis is reported. Simultaneous use of all three techniques is made possible by custom fitting a quartz glass window into the furnace of a commercially available TG-DTA. The quartz window enabled direct observations from a microscope mounted above the furnace throughout the entirety of the thermal analytical experiments. Several examples are provided for the use of this combined system for evaluating dehydrations, degradation and phase conversions in pharmaceutical materials. In some examples, microscopy provided information not accessible from the thermal analytical data alone. In others, the thermal analytical data was more informative than the microscopy.

Keywords: *hydrate, microscopy, polymorph, TG-DTA-microscopy, thermal analysis*

Introduction

Pharmaceutically active chemical entities are often isolated as a variety of differing polymorphic forms and/or as differing solvated/hydrated forms [1–4]. These differing solid-state forms of a drug substance may influence the stability, bioavailability, ease of manufacture and/or aesthetic appeal of the drug formulation [5]. As a result, efficient drug development and support of marketed drugs requires pharmaceutical scientists to fully understand the solid-state forms available for the medicinal compounds with which they work. Additionally, there is a regulatory expectation that the solid-state form be evaluated and as necessary, controlled [6].

The utility of thermal analysis to characterize and evaluate solid-state forms has long been recognized [3, 4] and recently the use of coupled thermal analytical techniques has also been described [7] as well as the use of DSC to quantitate differing solid-state forms [8]. The very recent use of DSC, TG and/or hot stage microscopy to characterize polymorphic forms of pharmaceutical actives and the thermodynamic relationship between forms is well documented [9–13]. The combination of differential scanning calorimetry with optical microscopy has been previously reported and called DSC photo-visual or DSC-thermal microscopy by some authors [14–16]. As reported, the simultaneous application of these two techniques enabled identification of phase transitions, interactions between formulation components and degradation onsets that would not have been possible using the techniques separately or via hot stage microscopy alone. The utility of combined DSC-microscopy is further demonstrated by the availability of a commercial DSC-microscopy instrument [17]. In this study, this approach is taken one step further. Microscopy is coupled to a commercial TG-DTA equipped with a quartz glass viewing window to allow simultaneous TG-DTA-microscopy. The utility and limitations of TG-DTA-microscopy to assist in solid-state characterization of pharmaceuticals is illustrated by several practical examples. The addition of the TG to the thermal microscopy experiment is shown to be particularly useful in interpretation of transitions related to desolvation.

Experimental

A commercially available Seiko SSC/5200 TG-DTA was modified with a double layer quartz window. The addition of the quartz glass window was demonstrated earlier to have no impact upon TG-DTA temperature calibration and baseline [18, 19]. This window provides a clear view of the sample and reference pans. The microscope, light and camera were placed above the furnace as shown in Fig. 1. To collect the sharpest pictures, the entire microscope could be moved vertically to the desired focus in addition to using the microscope focus adjustment. Visualization was optimized by increasing the depth of field by using a 0.5 objective combined with standard 10 times magnification eyepieces. Pictures were captured using the video software (Intervideo WinDVR3) with the same 5 times magnification achieved through the eyepieces. Ther-

* Author for correspondence: grundner.cl@pg.com

1388–6150/$20.00

Akadémiai Kiadó, Budapest, Hungary
Springer, Dordrecht, The Netherlands

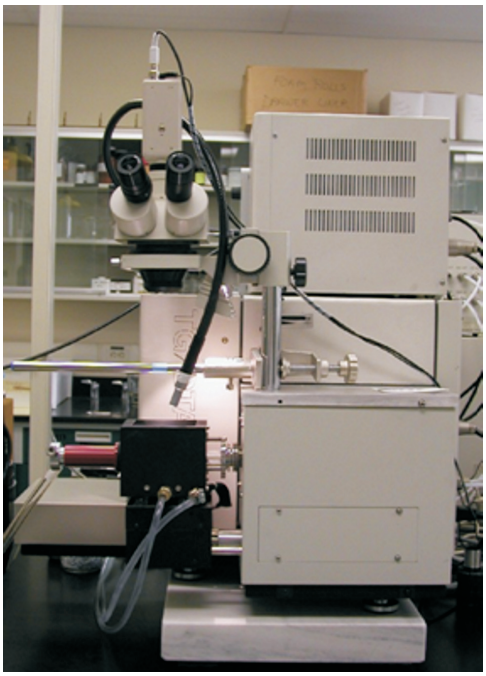

Fig. 1 Addition of a microscope, light and camera assembly to a modified TG/DTA

mal analysis experiments were visible through the microscope eyepieces as well as with the video software simultaneous with the TG-DTA scan. Pictures could be captured at critical points throughout the scan by manually operating the collection software.

Moderate intensity top lighting was required to obtain useable microscopy images. Baseline and temperature calibration checks were conducted to confirm that this top lighting did not interfere with either the TG or DTA responses. No change in baseline was observed with top lighting over the temperature range of interest (25 to 350°C). Additionally, a reference material containing a certified amount of water was used to further confirm the lack of interference from the top lighting. Sodium tartrate dihydrate was chosen as the reference material because the dehydration response expected for this material would be representative of the type of hydrates likely to be surveyed using the combined technique. As shown in Fig. 2, illumination did not impact the sample response and temperature. Samples of sodium tartrate were run at 5°C min^{-1} from 25 to 250°C with the light on and again with the light off. The DTA and TG sample response and temperature scans were separated and then overlaid for ease of comparison. No difference was observed between runs with and without illumination and the total mass loss observed matched the certified value for the reference material.

Experimental samples were run in open aluminum pans at the scan rate and sample size indicated with each example. A dry nitrogen purge was used to sweep the samples. The TG-DTA was temperature calibrated using gallium and tin.

DSC data were obtained using a TA 2920 at the scan rates noted in the discussion. Samples were enclosed in aluminum sample pans and run under dry nitrogen. The DSC was temperature calibrated using mercury, indium and lead, and heat flow calibrated using indium.

Results and discussion

Experimental compound EU-2972: visualization of a polymorphic transition

EU-2972 is an experimental compound known to exist in at least two different polymorphic forms. Based upon the Burger rules [3, 20], the two polymorphs observed in this study are monotropic. The less stable polymorph melts at a lower temperature than the more stable polymorph. When sufficient time is allowed, the more stable polymorph is observed to crystallize from the melt of the less stable form. This crystallization is observed as an exotherm located between the two melt endotherms. The relationship between the melts of the two forms and the crystallization exotherm is shown in Fig. 3 by a series of representa-

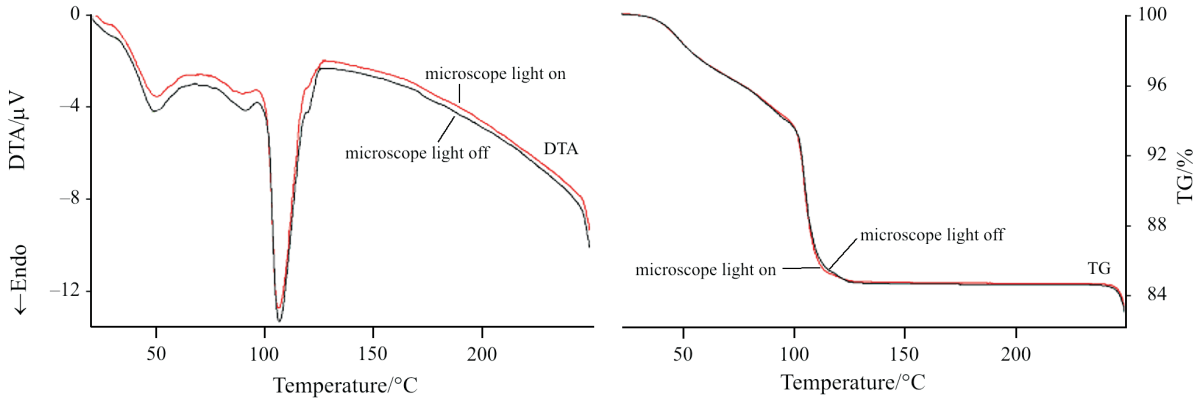

Fig. 2 DTA and TG signal of sodium tartrate showing that illumination does not impact the thermal responses

tive DSC thermal curves. Changing the scan rate from 20 to 40°C min^{-1} and finally to 60°C min^{-1} resulted in differing ratios of the two polymorphs as evidenced by the respective melts. The level of higher melting polymorph observed increased at slower scan rates, concurrently with an increase in the observed recrystallization exotherm. At slower scan rates, more time was available for crystallization of the more stable polymorph from the melt of the less stable polymorph, resulting in a larger melt endotherm for the stable form relative to the lower melting form.

The TG-DTA-microscope was used in an attempt to try to visually capture the three separate processes: melting of the less stable polymorph, crystallization to the more stable form and finally melting of the more stable polymorph. To increase chances of capturing the three events, the scan rate was reduced to 10°C min^{-1}. The resulting TG-DTA curve for a 6 mg sample is shown in Fig. 4. The characteristic endotherm, exotherm, endotherm pattern observed in the DSC experiments was observed here in the DTA

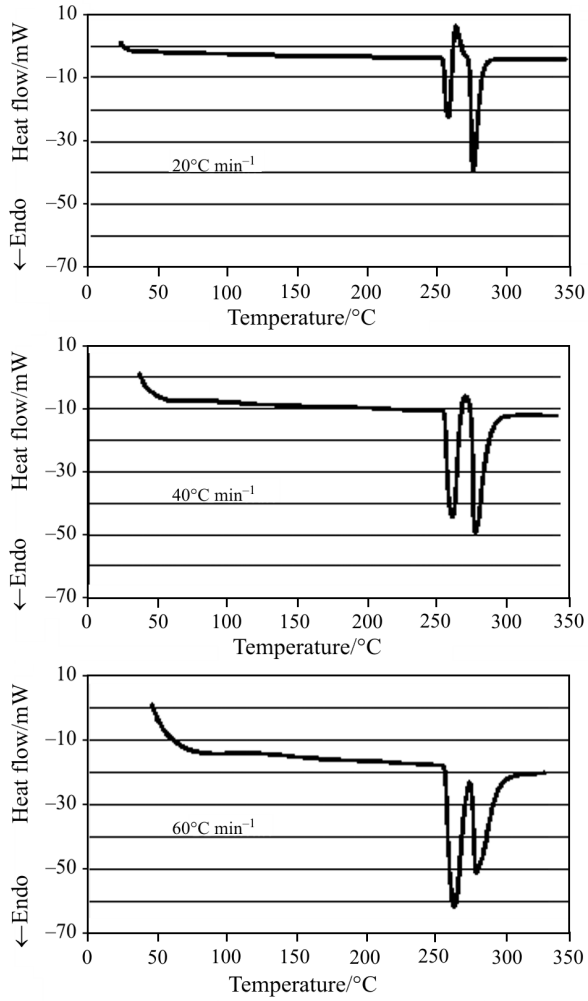

Fig. 3 Representative DSC curves for experimental compound EU-2972 illustrating impact of scan rate

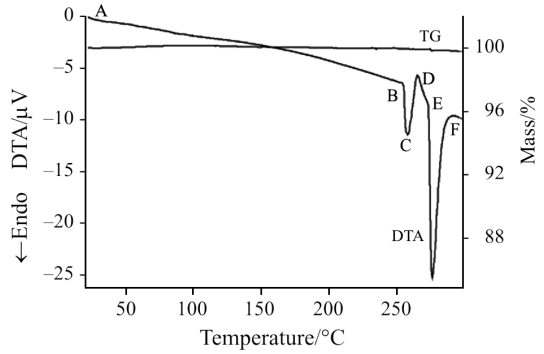

Fig. 4 Representative TG-DTA curve for experimental compound EU-2972

signal as expected. Addition of the TG data to the DSC and DTA results further confirmed the interpretation of the two endotherms as melts. No mass loss was observed throughout the scan. Mass loss may have been expected if either endotherm corresponded to degradation rather than melting.

The thermal curve for EU-2972 is labeled at key temperatures where photomicrographs were obtained and the corresponding photomicrographs are shown in Fig. 5. The photomicrographs provide additional information about the events occurring during the thermal scan, confirming the initial interpretation. At the start of the run, 25°C (A), the sample appearance was that of a whitish powder. At the onset of the first melt, 254°C (B), the sample took on a yellowish hue and became glassy or molten looking, initially just along the outside rim of the sample pan. As the melting of the less stable phase continued, the yellow, glassy looking front moved towards the center of the sample pan 258°C (C). By the time the melt front for the initial less stable phase had reached the center of the pan, crystallization of a more stable form was noted by the formation of an opaque, lighter colored solid originating at the outside rim of the pan and again moving towards the center 265°C (D). This time point coincides with the peak maximum for the observed exotherm. Photomicrograph D clearly shows the co-existence of the initial melt and the recrystallized forms in the same pan at the time the exotherm is observed in the thermal curve. By the onset of the second endotherm at 270°C (E), the more stable form had started to melt and by 300°C (F) was completely melted.

The photomicrographs not only support the earlier interpretation of the thermal curves but also show unequivocally that multiple transitions are occurring simultaneously within the sample pan. By the nature of the measurement, the TG, DSC or DTA signal must represent an overall average for the bulk material studied. Competing transitions cannot be readily deconvoluted. As shown in the series of DSC results,

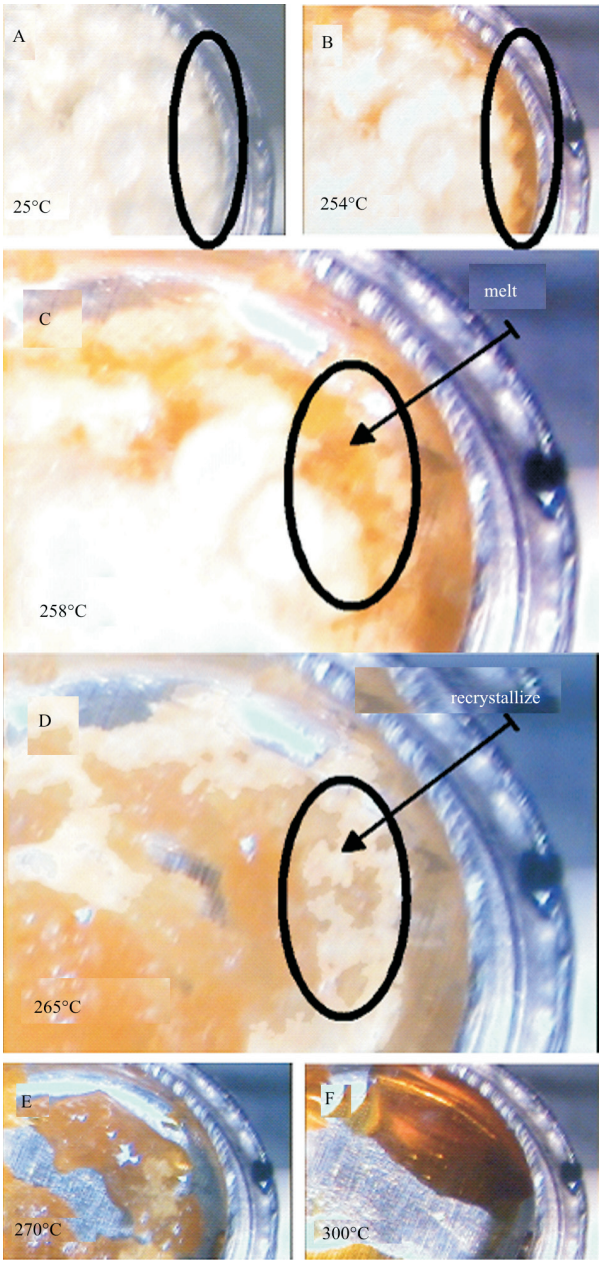

Fig. 5 Experimental compound EU-2972 photomicrographs: A – start of run, B – start of melt of less stable form, C – melt of less stable form progresses towards center of pan, D – recrystallization to a more stable form observed along pan edge, E – start of melt of stable form, F – complete melt of stable form

kinetic effects may sometimes be teased out using differing scan rates. By using the TG-DTA- Microscope, proof for the polymorphic conversion was obtained in a single scan. The photomicrographs illustrate how much less uniform the phase transitions are than might be imagined based upon the thermal analytical evidence alone. For instance, rather than observing the less stable polymorph melt simultaneously across the entire sample pan, the progression of the melt front is observed from pan edge to center as seen in photographs B through D in Fig. 5. Additionally, evidence for concurrent melt of the less stable polymorph with crystallization to the more stable form is readily seen in Photomicrograph D of Fig. 5 demonstrating the simultaneous presence of two competing transitions within the study sample.

Investigational compound A: lack of visual evidence for multiple phase transitions

Investigational Compound A is known to exist in both hydrated and anhydrous forms. Thermal curves obtained from this compound were complex so concurrent TG-DTA-Microscopy was evaluated as a tool for enhanced interpretation of the complicated TG-DTA curves. An 8 mg sample of the hydrate form of Compound A was scanned at 5°C min^{-1} from 25 to 280°C as shown in Fig. 6. The initial endotherm (A) and corresponding mass loss is consistent with the expected dehydration of the sample. The second smaller endotherm (B) may indicate a phase change (for example, melting of the now dried sample) or thermal degradation (although no mass loss is observed). The exotherm (C) observed above 100°C is suggestive of crystallization and supports the interpretation of B as a melt endotherm. The final endotherms (D, E) are consistent with either melting and/or degradation. Lack of mass loss associated with D suggests a melt. The small waver in the TG signal near E is consistent with a melt artifact observed in horizontal beam TGs due to sample motion on the lever arm. Above 200°C, both the endothermic DTA baseline and mass loss indicate sample degradation.

The TG-DTA curves illustrate at least six separate thermal events associated with heating Compound A. Although interpretations may be implied based upon some prior knowledge of the sample, additional data is required to positively identify each event. As shown in Fig. 7, the TG-DTA-Microscope provided only a minimum of information for this sample. No physical effects were apparent via microscopy

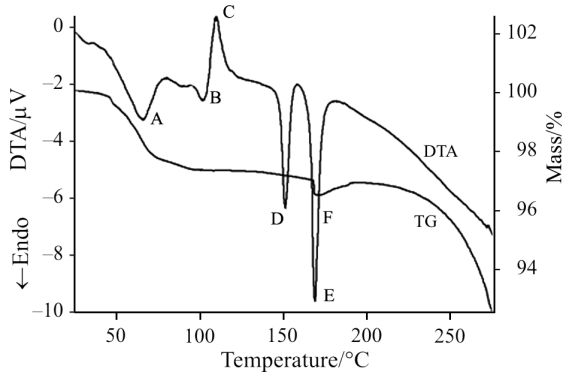

Fig. 6 Investigational compound A TG-DTA scan

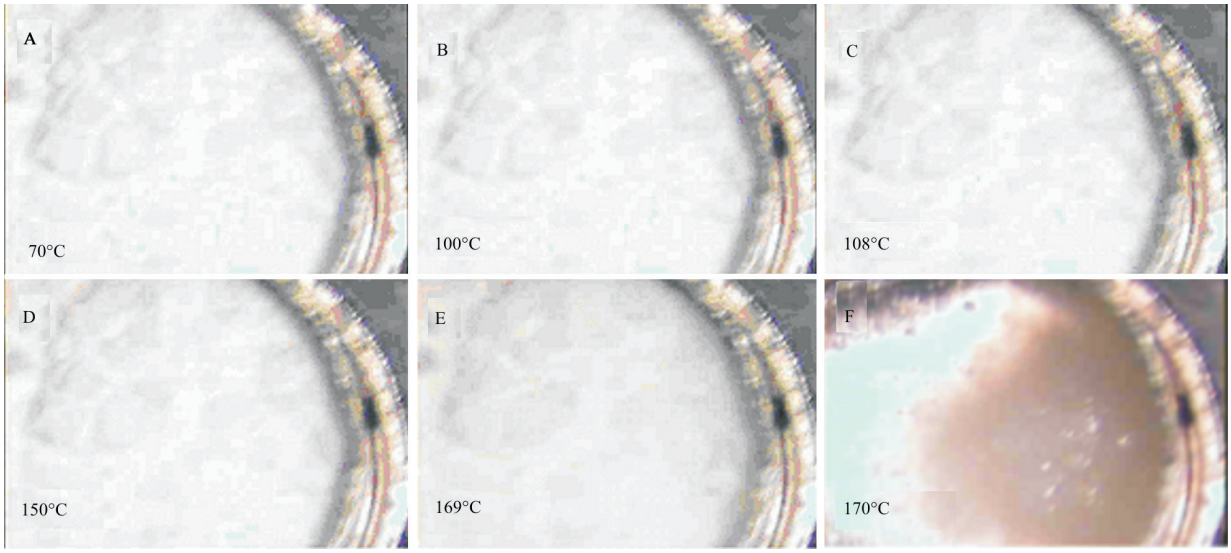

Fig. 7 Investigational Compound A photomicrographs: A – 1st endotherm, B – 2nd endotherm, C – exotherm, D – 3rd endotherm, E – 4th endotherm, F – end of 4th endotherm, melt

upon dehydration of the sample endotherm (A). If dehydration caused changes in crystal volume, hue or integrity, these changes were not apparent from visual observations. Similarly, no evidence of sample melting or recrystallization were observed during endotherm (B) and exotherm (C) although subsequent hot stage X-ray experiments did confirm this endotherm/exotherm pairing to be due to melt of the dried hydrate and crystallization to an anhydrate. No change in appearance was observed during endotherm D to aid in interpretation of this event. Development of this compound was suspended before a complete investigation and assignment of this thermal event could be made. The only obvious visual change observed for this sample occurred during endotherm (E). Sample melting, while not apparent at the endotherm minimum (E), was visually obvious upon completion of the last endotherm (F).

In this example, the TG-DTA-microscope did not significantly enhance interpretation capabilities beyond that of a TG-DTA. The difficulty in trying to observe differences in appearance of a finely divided, white powder is demonstrated as well as the limitations inherent in the use of hot stage microscopy of bulk samples. It is possible that a different combined technique such as TG-DTA-NIRA or TG-DTA- Raman may have been more useful in this example. Use of DSC-microscopy would be expected to be even less informative in this case as no information would have been gained relevant to the dehydration mass loss.

Risedronate: observation of the physical impact of dehydration and early detection of degradation

Risedronate monosodium is the active in the osteoporosis drug Actonel™. The thermal characterization of this compound and the differing hydration states available to Risedronate have previously been described [21–25]. Although a monohydrate form, variable hydrate and an anhydrate are known to exist, risedronate monosodium is marketed as a hemipentahydrate (2.5 moles of water). The dehydration, as monitored by thermal analysis, involves several distinct steps: loss of the first mole of channel water as a distinct TG step and DTA endotherm, gradual loss of half a mole of water noted only by a gradual decline in the TG baseline, loss of the final mole of water at higher temperatures as a distinct endotherm and mass loss, concurrent with crystallization of a portion of the material to a monohydrate form (observed by simultaneous spectroscopy techniques), then dehydration of the monohydrate (evidenced by a distinct endotherm and mass loss) followed by chemical degradation of the compound. Because of the complexity of the thermal signature for this compound it was evaluated to determine how concurrent microscopy could enhance interpretation of the observed thermal events.

The TG-DTA curves shown in Fig. 8 are representative of the thermal signature for a 5 mg sample obtained at 5°C min^{-1}. The initial mass loss and endotherm as previously reported [21, 23] are due to loss of one mole of channel type water of hydration. Channel type water of hydration is characterized by the relative ease with which dehydration may occur. Dehydration may occur spontaneously upon exposure to low relative humidity. Observations were made of a sample through dehydration of this mole of channel

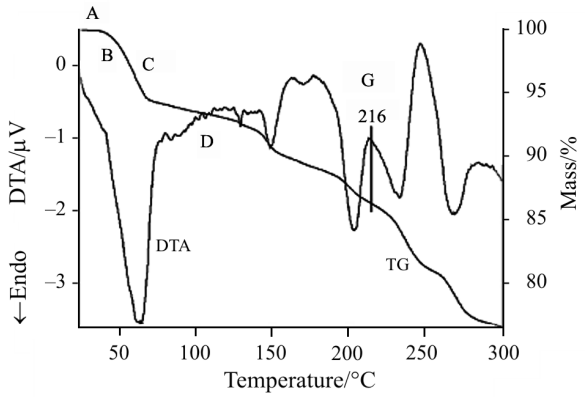

Fig. 8 Risedronate TG-DTA scan. Vertical line on thermal curve separates the mass losses due to dehydration from mass losses due to degradation

water to learn more about the physical consequences of the dehydration.

As shown in Fig. 9, the risedronate crystal visually appeared clear at 25°C (A), the start of the experiment. As mass loss due to dehydration initiated, 40°C (B), the crystal begin to grow opaque. The clouding of the crystal was due to stress fractures resulting from crystal lattice adjustments forced by the loss of channel water from the crystal. Confirmation of this interpretation was made via separate hot stage X-ray diffraction experiments that clearly showed lattice changes upon loss of this first mole of water. Upon further dehydration, 64°C (C), the crystal became more opaque and began to expand as the crystal lattice continued to adjust to accommodate the loss of water. Upon completion of the loss of the first mole of water, 70°C (D), the crystal was expanded as far as would be observed prior to degradation. The loss of the mole of channel water created stress fractures as result of the lattice reorganization in response to dehydration. In addition to microscopy and XRD studies, this change in lattice structure was confirmed by vibrational spectroscopies and solid-state NMR studies. Although several techniques were able to identify crystal lattice changes as a consequence of drying, only microscopy captured the physical consequence of drying, that of crystal fracturing. Follow up studies clearly demonstrated that this fracturing resulted in crystal size reduction whether drying was induced by heat or by low relative humidity. This information is critical to long term control of particle size distribution for the material.

As reported earlier [21–23], an additional one and a half moles of water are lost at higher temperatures, just prior to onset of degradation. Concurrent

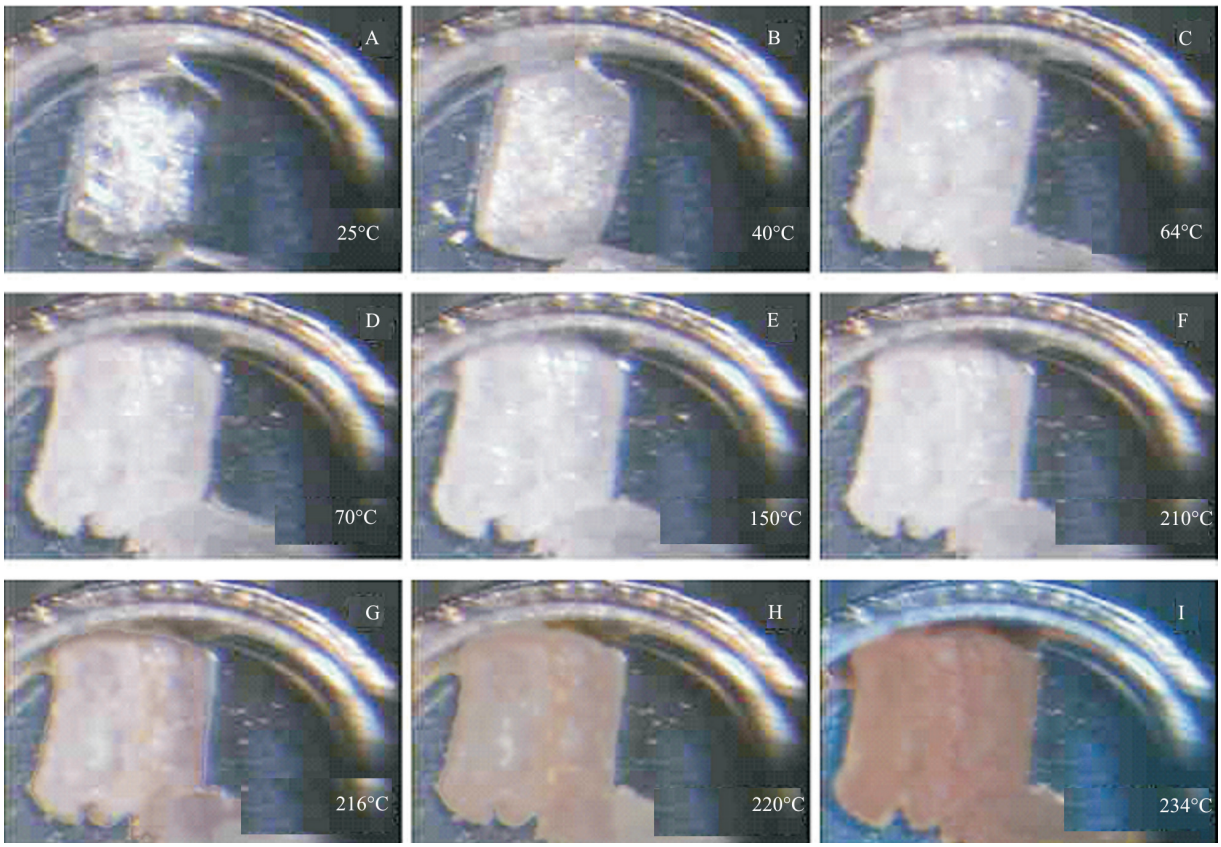

Fig. 9 Risedronate photomicrographs. Crystal fracturing upon dehydration observed (A) to (D). Onset of chemical degradation observed (G)

with the loss of the final mole of water of hydration, crystallization of a portion of the drying material to monohydrate has been reported through the use of simultaneous spectroscopy tools [24, 25]. Also, concurrently with the dehydration of the monohydrate that is formed in situ, anhydrate is crystallized [24, 25]. Overall, at the end of the dehydration scheme, final dehydration of the hemipentahydrate yields (non-quantitatively) monohydrate that in turn is dehydrated to form (again, non-quantitatively) anhydrate. Of interest was whether any of these events could be monitored by TG-DTA-microscopy. Even though multiple phase transitions were happening there were no obvious changes in crystal appearance from 70 to 210°C, the region over which these dehydrations and crystallizations are known to occur. The information provided by the microscope in this portion of the study is similar to the result for experimental Compound A. Visual effects were not observed during this region of the scan although dehydration and concurrent phase transitions occurred. The change in phase for the material was not visually evident.

Based upon the TG-DTA curves alone, it was difficult to assign a point for quantitation of total water loss for the sample. Multiple events from 150°C and higher might be considered. Use of the TG-DTA-microscope provided visual clues for separating onset of mass loss due to degradation from mass loss due to dehydration. Very slight yellowish orange discoloration was observed at the onset of degradation (G) with the color darkening as the temperature increased (H, I). Using this information to assign the endotherm starting at 216°C as the onset of visual degradation, the endotherm immediately preceding it (peaking near 200°C) may be interpreted as the final loss of water of hydration. Calculating from the TG inflection associated with this endotherm, a total water loss of 12.8% was determined. This value is in excellent agreement with 12.9%, the theory for a hemipentahydrate. Both Karl Fischer and X-ray single crystal structural assignments confirm that risedronate exists as the hemipentahydrate [21, 23]. In this example, while the microscopy did not provide information in relation to the higher temperature dehydrations, it did identify the onset of degradation, allowing for determination of total water of hydration.

Conclusions

Simultaneous TG-DTA-microscopy was shown to be useful in the characterization of pharmaceutical materials. As a survey tool for assessing polymorphs, phase transitions and dehydrations the combination of these three techniques provides advantages over the use of the techniques individually. Specifically, the addition of microscopy to the TG-DTA helped to confirm phase changes preliminarily assigned to EU-2972 based upon the DSC curves and clearly illustrated that multiple changes were occurring simultaneously within the same study sample. In another example, the microscopy portion of the experiment provided no significant assistance in interpretation of the particularly complex thermal curve of experimental Compound A, demonstrating the advantage of the combined technique over hot stage microscopy alone and reminding the researcher that significant physical and chemical changes may occur within a sample that do not result in any visual clues. In the case of Risedronate, microscopy showed the physical impact of the initial dehydration, information that could not be gained from the thermal data alone. In addition, microscopy provided data to assist in determination of the temperature that marked the end of dehydration and onset of degradation, allowing for quantitation of water of hydration.

References

1 J. K. Haleblian and W. J. McCrone, J. Pharm. Sci., 58 (1969) 911.
2 J. K. Haleblian, J. Pharm. Sci., 64 (1975) 1269.
3 D. Giron, Thermochim. Acta, 248 (1995) 1.
4 H. G. Brittain Ed., 'Polymorphism in Pharmaceutical Solids', Marcel Dekker, Inc., New York 1999.
5 G. G. Z. Zhang, D. Law, E. A. Schmitt and Y. Qiu, Adv. Drug Deliv. Rev., 56 (2004) 372.
6 D. Giron, M. Mutz and S. Garnier, J. Therm. Anal. Cal., 77 (2004) 709.
7 D. Giron, J. Therm. Anal. Cal., 68 (2002) 335.
8 I. M. Vitéz, J. Therm. Anal. Cal., 78 (2004) 33.
9 U. J. Griesser, D. Weigand, J. M. Rollinger, M. Haddow and E. Gstrein, J. Therm. Anal. Cal., 77 (2004) 511.
10 M. R. Caira, A. Foppoli, M. E. Sangalli, L. Zema and F. Giordano, J. Therm. Anal. Cal., 77 (2004) 653.
11 M. R. Caira, S. A. Bourne and C. L. Oliver, J. Therm. Anal. Cal., 77 (2004) 597.
12 E. V. Boldyreva, V. A. Drebushchak, I. E. Paulkov, Y. A. Kovalevskaya and T. N. Drebushchak, J. Therm. Anal. Cal., 77 (2004) 607.
13 S. Pfeffer-Hennig, P. Poechon, M. Bellus, C. Goldbronn and E. Tedesco, J. Therm. Anal. Cal., 77 (2004) 663.
14 C. F. S. Arãgao, J. M. B. Filho and R. O. Macedo, J. Therm. Anal. Cal., 64 (2001) 185.
15 F. S. de Souza, A. P. G. Barreto and R. O. Macedo, J. Therm. Anal. Cal., 64 (2001) 739.
16 R. O. Macedo, T. G. do Nascimento and J. W. E. Veras, J. Therm. Anal. Cal., 67 (2002) 483.
17 M. Wagner and M. Schubnell, Proceedings of the 32nd NATAS Conference, 2004, p. 122.
18 W. J. Collins, C. DuBois, R. T. Cambron and N. L. Redman-Furey, Proceedings of the 31st NATAS Conference, 2003.

19 W. J. Collins, R. T. Cambron, N. Redman-Furey and A. Bigalow-Kern, J. ASTM Int., 2 (2005) JAI 12789.
20 B. Burger, Acta Pharm. Technol., 28 (1982) 1.
21 N. L. Redman-Furey, W. J. Collins and M. A. Burgin, Proceedings of the 30th NATAS Conference, 2002, p. 733.
22 N. L. Redman-Furey, M. L. Dicks, J. Godlewski, D. C. Vaughn and W. J. Collins, J. ASTM Int., 2 (2005) JAI 12972.
23 N. L. Redman-Furey, M. Dicks, A. S. Bigalow-Kern, R. T. Cambron, G. Lubey, C. Lester and D. Vaughn, J. Pharm. Sci., 94 (2005) 893.
24 A. S. Bigalow-Kern, R. T. Cambron, W. J. Collins, C. DuBois and N. L. Redman-Furey, J. ASTM Int., 2 (2005) JAI 12790.
25 A. S. Bigalow-Kern, K. B. Poiesz, R. T. Cambron, C. L. Grundner and N. L. Redman-Furey, Proceedings of the 33rd NATAS Conference, 2005.

DOI: 10.1007/s10973-005-7352-x